

Self-Assembly of Russian Doll Concentric Porphyrin Nanorings

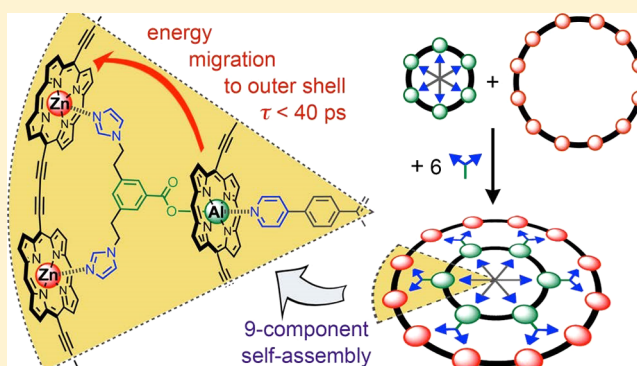
Sophie A. L. Rousseaux,[†] Juliane Q. Gong,[‡] Renée Haver,[†] Barbara Odell,[†] Tim D. W. Claridge,[†] Laura M. Herz,[‡] and Harry L. Anderson^{*,†}

[†]Department of Chemistry, University of Oxford, Chemistry Research Laboratory, Oxford OX1 3TA, United Kingdom

[‡]Department of Physics, University of Oxford, Clarendon Laboratory, Oxford OX1 3PU, United Kingdom

Supporting Information

ABSTRACT: Electronic communication between concentric macrocycles with wave functions that extend around their circumferences can lead to remarkable behavior, as illustrated by multiwalled carbon nanotubes and photosynthetic chlorophyll arrays. However, it is difficult to hold one π -conjugated molecular ring inside another. Here, we show that ring-in-ring complexes, consisting of a 6-porphyrin ring locked inside a 12-porphyrin ring, can be assembled by placing different metals in the two rings (zinc and aluminum). A bridging ligand with carboxylate and imidazole binding sites forms spokes between the two rings, resulting in a highly cooperative supramolecular self-assembly process. Excitation is transferred from the inner 6-ring to the outer 12-ring of this Russian doll complex within 40 ps. These complexes lead to a form of template-directed synthesis in which one nanoring promotes formation of a larger concentric homologous ring; here, the effective template is an eight-component noncovalent assembly. Russian doll templating provides a new approach to amplifying the size of a covalent nanostructure.



INTRODUCTION

Hierarchical ring-in-ring assemblies, such as Russian doll complexes, have intrigued supramolecular chemists for over a decade.^{1–4} Russian dolls are nested assemblies of self-similar objects such that the shells form a homologous series. When a macrocyclic receptor undergoes role reversal and becomes encapsulated by a larger ring, this can fundamentally change its dynamics and chemical behavior. Russian dolls consisting of concentric π -conjugated macrocycles, or rings of chromophores, are fascinating systems in which to study the flow of electronic excitation and charge.^{1f,5} We and others have recently reported the synthesis of π -conjugated macrocycles consisting of covalently linked porphyrin units that exhibit ultrafast energy migration and that mimic the photophysical behavior of natural photosynthetic antenna systems.^{6–10} In purple bacteria, sunlight is captured by two circular light harvesting (LH) complexes, LH1 and LH2, which are rings of chlorophyll molecules. Excitation energy is funneled from LH2 to LH1, where it is transferred to the reaction center (RC), which is nested within the LH1 ring.¹¹ Here, we demonstrate that two nanorings, consisting of 6- and 12-porphyrin units, respectively, self-assemble in the presence of an appropriately designed bridging ligand to exclusively yield a Russian doll complex reminiscent of the LH1-RC architecture (Figure 1). This nine-component self-assembly process involves four types of subunits, which can be mixed together in any order. It is driven by the complementary metal–ligand interactions present in the two ring components: the inner 6-porphyrin nanoring

has aluminum(III) metal centers, which selectively bind carboxylate ligands, whereas the outer 12-porphyrin nanoring has zinc(II) centers, which coordinate nitrogen-containing ligands such as imidazoles.^{12,13} Time-resolved photophysical experiments show that the Russian doll complex behaves as a single emitter and that excitation is transferred outward, from the inner 6-porphyrin nanoring to the outer 12-porphyrin ring. Finally, we demonstrate that the smaller 6-porphyrin ring can be used as a template to direct the synthesis of the 12-porphyrin nanoring. Thus, Russian doll templating provides a way to escalate the size of these covalent nanostructures.

RESULTS AND DISCUSSION

Our design for the ring-in-ring structure is illustrated in Figure 1, and the individual components for its assembly are shown in Figure 2. The outer ring *c*-P12, which was prepared using Vernier templating,^{6a} contains zinc-porphyrins that bind amines such as pyridine and imidazole. For the inner 6-porphyrin ring, we chose aluminum-porphyrins because they bind complementary oxygen-containing ligands such as carboxylates or phenolates. Al-porphyrins can also form hexacoordinate complexes on binding pyridine ligands.^{13b,c} Thus, we imagined that 1 equiv of the hexapyridyl template T6 could nest within the aluminum 6-ring, forcing the bridging ligands to reside on the external surface for coordination to *c*-P12.

Received: August 11, 2015

Published: September 17, 2015

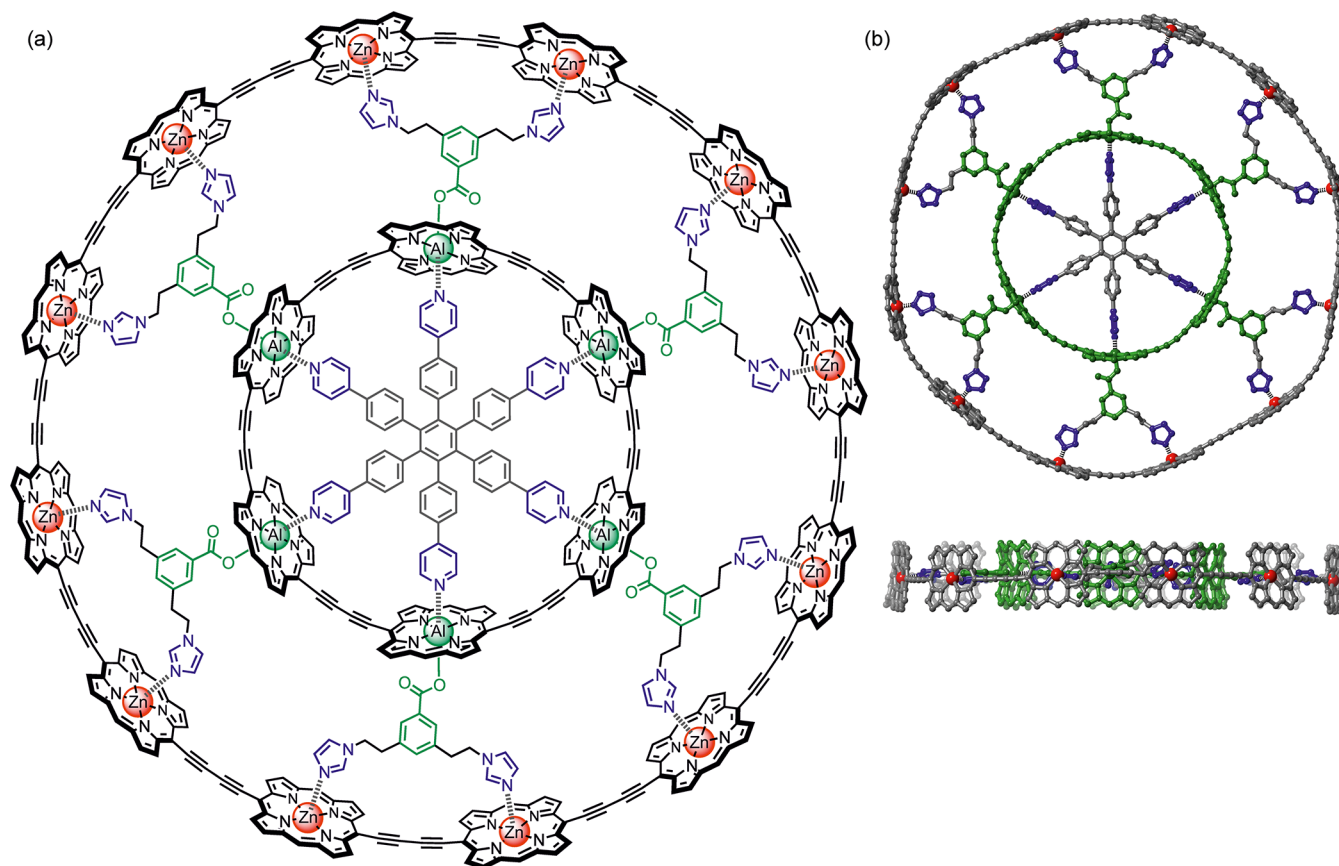


Figure 1. Structure of the Russian doll complex. (a) Chemical structure (with *meso*-aryl side groups omitted for clarity). (b) Two orthogonal views of the calculated structure. (MM+ force field, HyperChem; *meso*-aryl side groups were not included in the calculations; hydrogen atoms were omitted for clarity).

We used molecular mechanics calculations to screen a variety of Y-shaped ligands, designed to act as spokes and to bridge between the two nanorings (Figure 1). Ligand L1 was found to have the most suitable geometry; it contains two imidazole groups, to bind the zinc-porphyrin nanoring, and a carboxylate, to bind aluminum (Figure 2c).

Synthesis of the Aluminum 6-Porphyrin Nanoring.

Hexacoordinate Al-porphyrins form interesting self-assembled structures due to their ability to bind both carboxylate and nitrogen-containing ligands. However, they remain poorly exploited for this purpose due to their challenging synthesis and purification.¹³ The Al-nanoring complex T6·c-P6·(Ar'CO₂)₆ was prepared in three steps from the corresponding zinc-porphyrin nanoring.^{6b} Treating this zinc nanoring with excess trifluoroacetic acid yielded the free-base porphyrin nanoring, which was then remetallated using AlMe₃ and finally isolated as T6·c-P6·(Ar'CO₂)₆ (see the Supporting Information for experimental procedures). The use of a capping carboxylate ligand (Ar'CO₂, i.e., 3,5-dimethylbenzoate) was necessary to avoid the formation of insoluble material because the hydroxoderivative c-P6·(OH)₆ gradually polymerizes in solution, presumably via formation of Al–O–Al links.

The hexapyridyl template T6 forms a 1:1 complex with the aluminum porphyrin nanoring c-P6·(Ar'CO₂)₆. Simply mixing solutions of the two components at room temperature for 30 min leads to the quantitative formation of the template complex T6·c-P6·(Ar'CO₂)₆. This complex can be purified by size-exclusion chromatography, whereas before insertion of T6, the

aluminum porphyrin intermediates are not stable to chromatography.

Self-Assembly and Characterization of the Russian Doll Complex. The formation of the ring-in-ring structure was monitored by ¹H NMR spectroscopy, by titrating ligand L1 into a 1:1 mixture of c-P12 and T6·c-P6·(Ar'CO₂)₆ in CD₂Cl₂ (Figures 3a and S1). Although the aluminum porphyrins in T6·c-P6·(Ar'CO₂)₆ are capped with carboxylate ligands (Ar'CO₂), we expected that ligand exchange would occur,^{13b} resulting in replacement of these carboxylic acids with L1. Because this process is reversible, the formation of the Russian doll complex should act as a thermodynamic sink. Indeed, upon addition of 6 equiv of L1 to the 1:1 mixture of rings, the system equilibrates to a single product.

The ¹H NMR spectrum of the Russian doll complex, after purification by size-exclusion chromatography to remove the free capping ligand Ar'CO₂H, is shown in Figure 3b. The complex is highly symmetric, which facilitates the interpretation of its spectrum (see the Supporting Information for the detailed assignment). In the NOESY spectrum, a path of nuclear Overhauser effects connects the inner 6-ring and outer 12-ring (Figure 3b). NOEs are observed from the protons of the *tert*-butyl group on the aryl side groups in c-P6 to ligand protons k, m, and n. There are also NOEs n ↔ o, o ↔ p, p ↔ a, and p ↔ b, confirming the proximity of the two nanorings.

The properties of the Russian doll complex were compared with those of a 1:1 mixture of T6·c-P6·(Ar'CO₂)₆ and c-P12·(Bn-L1)₆. We call this reference sample the control mix; it contains the same elements as the Russian doll, but the benzyl

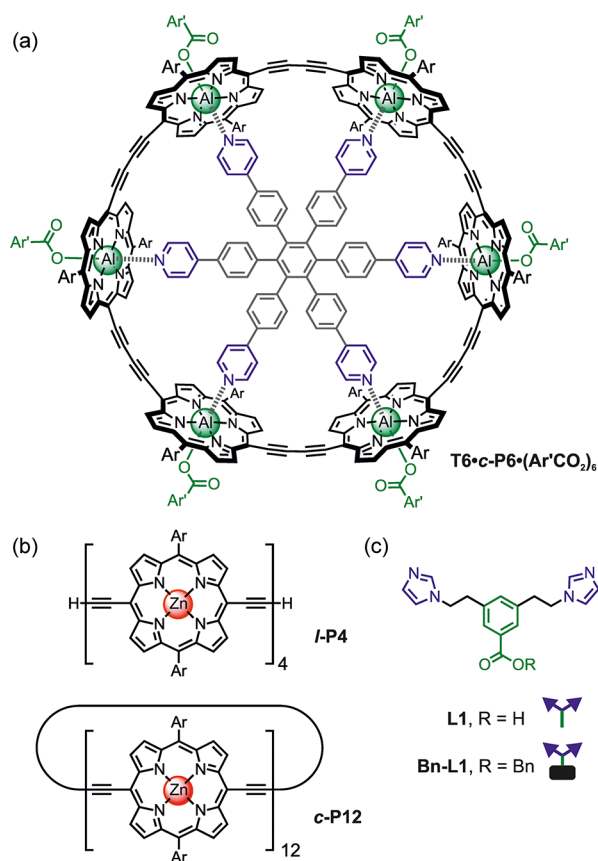


Figure 2. Chemical structures and schematic representations of the individual components used throughout this study. (a) Aluminum nanoring complex $T6 \cdot c-P6 \cdot (Ar'CO_2)_6$. (b) Zinc linear tetramer $l-P4$ and nanoring $c-P12$. (c) Bridging ligand $L1$ and its benzyl-protected derivative, $Bn-L1$. $Ar = 3,5$ -bis(*tert*-butyl)phenyl or $3,5$ -bis(octyloxy)phenyl; $Ar' = 3,5$ -dimethylphenyl.

ester-protecting group in $Bn-L1$ prevents formation of a ring-in-ring complex. The 1H NMR spectrum of the control mix differs significantly from that of the Russian doll complex, especially in the region of the porphyrin protons (Figure 4a,b). As expected, the β -pyrrole protons of $c-P12$ are split in the Russian doll, so that proton a is not equivalent to d and proton b is not equivalent to c , due to the binding mode of ligand $L1$ (Figure 3b). The aluminum 6-ring protons are shielded when the 6-ring binds inside the 12-ring, as expected from the ring currents of the porphyrin units.

Diffusion-ordered NMR spectroscopy (DOSY) experiments confirmed the formation of the ring-in-ring Russian doll, compared to the control mix (Figure 4c,d).¹⁴ The control mix clearly contains two separate rings that diffuse independently. The smaller ring $T6 \cdot c-P6 \cdot (Ar'CO_2)_6$ (green signals) has a diffusion coefficient of $(3.11 \pm 0.12) \times 10^{-10} \text{ m}^2/\text{s}$, whereas the larger ring $c-P12 \cdot (Bn-L1)_6$ (red signals) has a diffusion coefficient of $(2.29 \pm 0.03) \times 10^{-10} \text{ m}^2/\text{s}$. In the Russian doll, both rings diffuse at the same rate, which provides strong evidence that the smaller ring is fixed inside the larger ring. The diffusion coefficient of the Russian doll is $(2.29 \pm 0.03) \times 10^{-10} \text{ m}^2/\text{s}$, which is identical to that of $c-P12 \cdot (Bn-L1)_6$. These diffusion coefficients show that the hydrodynamic radii are dominated by the external $c-P12$ ring, despite the difference in molecular weight of approximately 5 kDa.

To further examine the self-assembly of the ring-in-ring structure, the control mix was treated with ligand $L1$. The

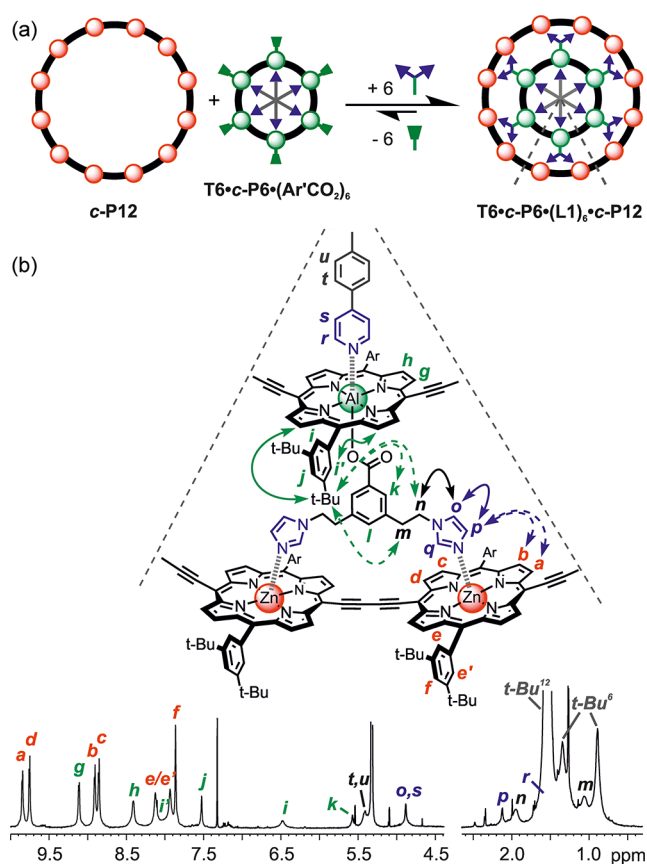


Figure 3. Self-assembly and 1H NMR spectrum of the Russian doll complex. (a) Assembly of the Russian doll complex from a 1:1 mixture of $c-P12$ and $T6 \cdot c-P6 \cdot (Ar'CO_2)_6$ in the presence of ligand $L1$. (b) 1H NMR spectrum (CD_2Cl_2 , 400 MHz, 298 K) and signal assignment for the complex (red letters, protons on $c-P12$; green letters, protons on $c-P6$ and the carboxylate part of $L1$; blue letters, protons on the imidazole and pyridine groups). Selected NOEs between nanoring and ligand protons are indicated by arrows (dotted arrows, weak NOEs; full arrows, strong NOEs).

changes in product distribution were monitored by 1H NMR titration. Despite the presence of 6 equiv of $Bn-L1$ in the control mix, which compete for binding to $c-P12$, the entire mixture rapidly equilibrates to the Russian doll complex (Figure S5).

The cooperativity of the self-assembly process was evaluated by comparing the stability of the Russian doll complex and $c-P12 \cdot (Bn-L1)_6$ toward denaturation by adding quinuclidine to break up the complexes.^{15,16} These denaturation processes were monitored by UV-vis-NIR spectroscopy (Figure 5). Reference titrations showed that quinuclidine does not displace $T6$ from $T6 \cdot c-P6 \cdot (Ar'CO_2)_6$ under these conditions. The concentration of quinuclidine required to break up the Russian doll complex $T6 \cdot c-P6 \cdot (L1)_6 \cdot c-P12$ into its component nanorings, $T6 \cdot c-P6 \cdot (L1)_6$ and $c-P12$, is about 6 mM, compared to 0.03 mM for dissociation of $c-P12 \cdot (Bn-L1)_6$ into $c-P12$ and $Bn-L1$. This 200-fold difference in sensitivity to quinuclidine reflects the chelate cooperativity of the Russian doll structure. The titration of the Russian doll with quinuclidine is essentially isosbestic, suggesting that it can be modeled as a two-state equilibrium. However, the binding isotherm is less sigmoidal than expected for an all-or-nothing process with this stoichiometry, as can be seen by comparing the experimental and calculated isotherms (Figure S6).¹⁵ The onset of

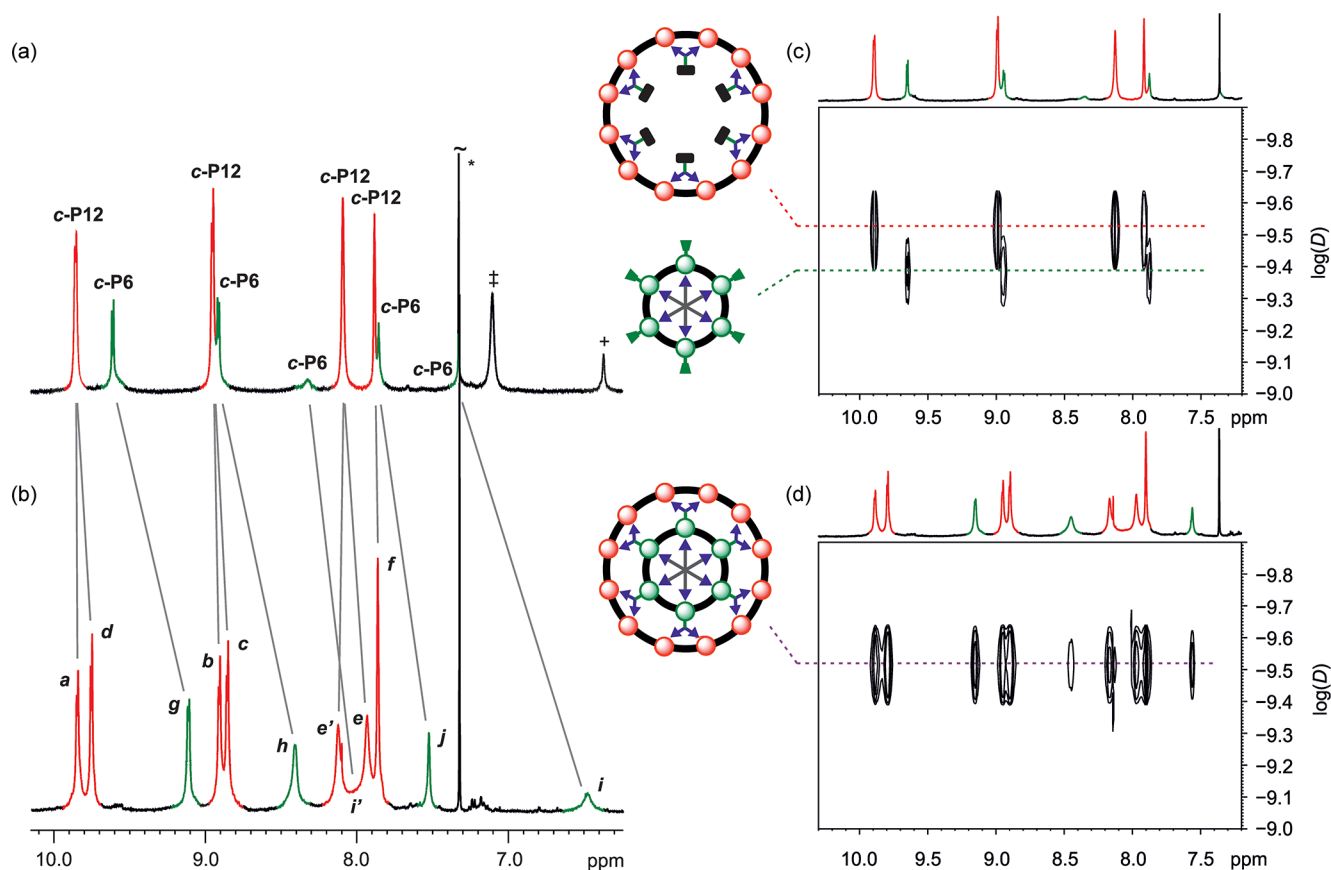


Figure 4. Comparison of NMR spectra of the control mix and the Russian doll complex (400 MHz, CD_2Cl_2 , 298 K). (a) ^1H NMR spectrum of the control mix made from a 1:1 mixture of $\text{T6}\cdot\text{c-P6}\cdot(\text{Ar}'\text{CO}_2)_6$ (green signals) and $\text{c-P12}\cdot(\text{Bn-L1})_6$ (red signals). (b) ^1H NMR spectrum of the Russian doll sample. Labels refer to the protons highlighted in Figure 3. The change in chemical shifts (and loss of symmetry) that are observed upon forming the complex are shown with gray lines. (c) DOSY ^1H NMR of the control mix where the two rings diffuse separately. (d) DOSY ^1H NMR of the Russian doll sample where the entire mixture diffuses as a single complex. The y-axis in (c) and (d) is the logarithm of the diffusion coefficient (D , $\text{m}^2 \text{s}^{-1}$). * indicates residual CHCl_3 ; ‡ indicates protons from the benzyl ester group in $\text{c-P12}\cdot(\text{Bn-L1})_6$; + indicates the para proton from 3,5-dimethylbenzoate in $\text{T6}\cdot\text{c-P6}\cdot(\text{Ar}'\text{CO}_2)_6$.

denaturation, at low quinuclidine concentrations, is more gradual than expected, indicating that partially bound species build up to significant concentrations. Denaturation of the Russian doll complex is highly cooperative (Hill coefficient: $n_{\text{H}} = 3.9$), but it is less cooperative than expected for an all-or-nothing process ($n_{\text{H}} = 8.0$).¹⁶ Although the simple two-state 12-site model does not give a perfect fit to the data, we can use this model to estimate the stability of the complexes. This model gives an equilibrium constant of $K_{\text{dn}} = (9.6 \pm 3.0) \times 10^{19} \text{ M}^{-11}$ for denaturation of the Russian doll complex.¹⁵ In the case of $\text{c-P12}\cdot(\text{Bn-L1})_6$, fitting to a 2-site binding model gives $K_{\text{dn}} = (2.5 \pm 0.2) \times 10^3 \text{ M}^{-1}$. These values imply that the decadic logarithm of the 1:1 equilibrium constant for formation of the Russian doll from $\text{T6}\cdot\text{c-P6}\cdot(\text{L1})_6$ and c-P12 is $\log K_{\text{f}} = 40 \pm 1$ and that the average effective molarity for Russian doll formation is about 1 M ($\log \overline{\text{EM}} = -0.1 \pm 0.2$; see Supporting Information for details of this calculation). The deviation from all-or-nothing behavior observed during denaturation of $\text{T6}\cdot\text{c-P6}\cdot(\text{L1})_6\cdot\text{c-P12}$ is probably a consequence of the modest effective molarity; similar behavior was reported previously in denaturation of a 24-porphyrin nanoring DABCO complex.¹⁷

Energy Migration. The absorption and fluorescence spectra of the Russian doll complex were compared with those of reference compounds (in chloroform at 295 K) to

explore the interactions between the two nanoring components.

The absorption spectra of porphyrin nanorings consist of a B band (400–550 nm) and a Q-band (650–950 nm). Nanorings c-P6 and c-P12 have similar B bands, whereas the Q-band of c-P12 is shifted to longer wavelengths. Comparison of the absorption spectrum of the Russian doll complex $\text{T6}\cdot\text{c-P6}\cdot(\text{L1})_6\cdot\text{c-P12}$ with that of $\text{c-P12}\cdot(\text{Bn-L1})_6$ (Figure S40) shows that the Q-band of the Russian doll is red-shifted and more intense, which indicates that the c-P12 component in the Russian doll is held in a more rigid and conjugated conformation.¹⁸ The same effect is evident in the fluorescence spectra (Figure S41): the Russian doll gives a peak emission of 928 nm, compared with 917 nm for $\text{c-P12}\cdot(\text{Bn-L1})_6$.

The fluorescence excitation spectrum of the Russian doll matches perfectly with its absorption spectrum (Figure S42), and its fluorescence lifetime (370 ps) is independent of excitation wavelength (Figure S43), which demonstrates that there is rapid energy migration between the nanoring components and that the whole supramolecular assembly behaves as a single emitter. In contrast, the control mix has an excitation spectrum that is different from its absorption spectrum and a fluorescence lifetime that changes with excitation wavelength because it consists of two independent species with different absorption spectra, different fluorescence

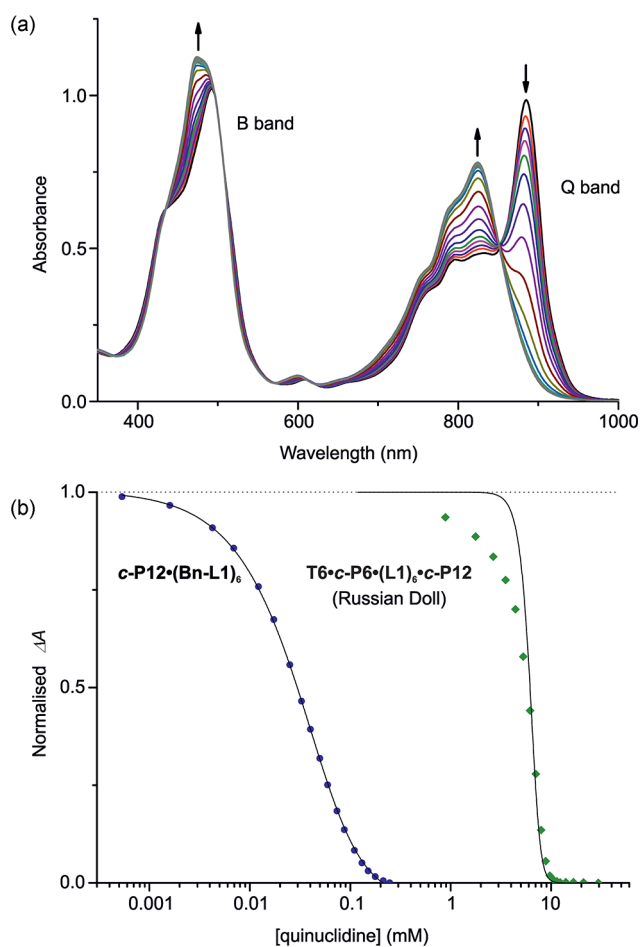


Figure 5. Denaturation titration of the Russian doll complex. (a) UV–vis–NIR titration of the Russian doll ($c = 6.05 \times 10^{-7}$ M) with quinuclidine (CHCl_3 , 298 K). Changes in absorption upon addition of quinuclidine are indicated by arrows. (b) Binding isotherms for the denaturation of the Russian doll complex (green dots, derived from absorption data at 885 nm) and $c\text{-P12}(\text{Bn-L1})_6$ (blue dots, derived from absorption data at 849 nm). The calculated fits are indicated by black lines.

quantum yields, and different fluorescence lifetimes. The emission profiles of the aluminum 6-ring and zinc 12-ring overlap significantly, which makes it difficult to study the energy migration dynamics in this system, but it is clear that excitation is transferred efficiently from the inner $c\text{-P6}$ component to the outer $c\text{-P12}$ component within the 40 ps time resolution of our instrumentation (time-correlated single-photon counting).

Russian Doll Templating. Radial oligopyridine ligands are effective templates for directing the synthesis of cyclic zinc-porphyrin oligomers.^{6,17,19} The successful assembly of the Russian doll complex led us to wonder whether the aluminum 6-ring, in combination with ligand **L1**, might act as a template for directing the formation of $c\text{-P12}$. In principle, this strategy offers a layer-by-layer approach to constructing even larger Russian dolls.

To test the viability of ring-around-ring templating, linear zinc-porphyrin tetramer $I\text{-P4}$ (Figure 2b) was added to a solution containing $\text{T6}\cdot c\text{-P6}\cdot(\text{Ar}'\text{CO}_2)_6$ and ligand **L1** (Figure 6a). The mixture was then submitted to standard palladium-catalyzed alkyne coupling conditions.^{6,17,19c–e} As a control reaction, $I\text{-P4}$ was also coupled in the presence of $\text{T6}\cdot c\text{-P6}\cdot$

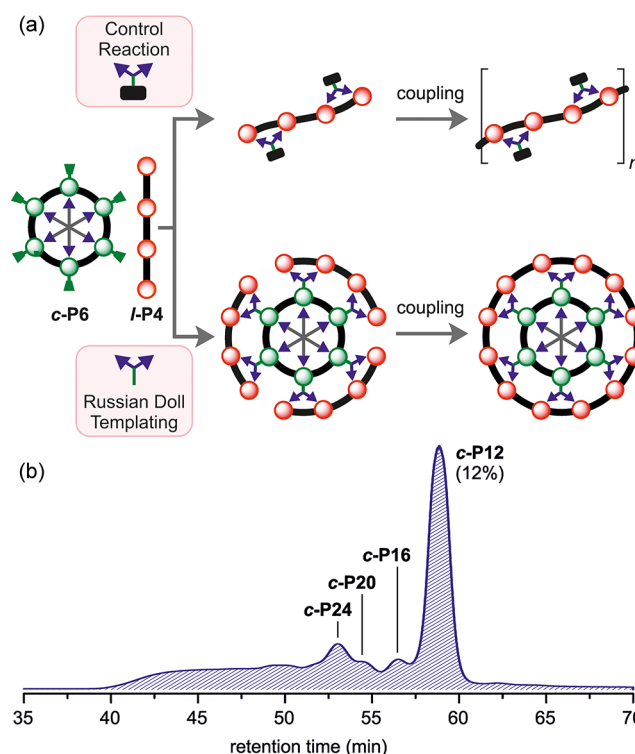


Figure 6. Reaction design and outcome of Russian doll templating for the synthesis of $c\text{-P12}$. (a) Schematic representation of the control reaction and the Russian doll templating synthesis of $c\text{-P12}$ around $\text{T6}\cdot c\text{-P6}\cdot(\text{Ar}'\text{CO}_2)_6$. (b) GPC trace (toluene/1% pyridine) of the Russian doll templating reaction product mixture after removal of the template $\text{T6}\cdot c\text{-P6}\cdot(\text{L1})_6$. Products were identified by analytical GPC, based on calibrated retention times, MALDI-TOF, and ^1H NMR for $c\text{-P12}$ and $c\text{-P24}$. The aryl solubilizing side group in $c\text{-P12}$ is $\text{Ar} = 3,5\text{-bis}(\text{octyloxy})\text{phenyl}$.

$(\text{Ar}'\text{CO}_2)_6$ and ligand **Bn-L1**, where the presence of a benzyl ester protecting group blocks the formation of a Russian doll complex. After the coupling reactions, insoluble polymers were removed on a short alumina column and the template $\text{T6}\cdot c\text{-P6}\cdot(\text{L1})_6$ was separated from the zinc-porphyrin oligomers by passing the reaction mixtures over a size-exclusion column in $\text{CHCl}_3/10\%$ pyridine. The reaction products were identified by analytical GPC, based on calibrated retention times,^{6c} MALDI-TOF analysis, and ^1H NMR spectroscopy for $c\text{-P12}$ and $c\text{-P24}$. As expected, the control reaction led to (mostly insoluble) polymer (Figure S45). In the Russian doll templating reaction, $I\text{-P4}$ was converted to $c\text{-P12}$ in 12% yield (measured by GPC; Figure 6b); here, the effective template is a noncovalent assembly of eight components. Besides the formation of the expected product ($c\text{-P12}$) from classical templating, the products resulting from Vernier templating ($c\text{-P24}$)^{6a,17} and caterpillar track templating^{19e} ($c\text{-P16}$ and $c\text{-P20}$) were also isolated. Russian doll templating represents a new approach for the synthesis of a large ring, using a smaller homologous ring as a template. The number of components (11 in total) that must successfully assemble in this synthesis of $c\text{-P12}$ from $I\text{-P4}$ demonstrates the power of self-assembly for the synthesis of large structures from simple components.^{6c,20}

CONCLUSIONS

A Russian doll complex of two porphyrin nanorings has been prepared via a nine-component self-assembly process. Four

categories of components, including a zinc porphyrin 12-ring, an aluminum porphyrin 6-ring, bifunctional bridging ligands, and a hexapyridyl template, selectively associate to yield a supramolecular complex reminiscent of the chlorophyll arrays in photosynthetic bacteria, with a molecular weight of 17 kDa. The ring-in-ring structure was confirmed by a series of NMR and photophysical experiments. The latter revealed that quantitative energy migration occurs within 40 ps, from the 6-ring to the 12-ring. The formation of this nested structure was also exploited for the development of Russian doll templating, where the smaller ring serves as a template for the covalent synthesis of a ring with twice its diameter.

■ ASSOCIATED CONTENT

● Supporting Information

The Supporting Information is available free of charge on the ACS Publications website at DOI: 10.1021/jacs.5b07956.

Synthetic procedures, characterization data, binding studies, NMR assignments, photophysics, and details of the template-directed synthesis (PDF).

■ AUTHOR INFORMATION

Corresponding Author

*harry.anderson@chem.ox.ac.uk

Notes

The authors declare no competing financial interest.

■ ACKNOWLEDGMENTS

We thank the European Research Council (grant 320969), the EPSRC, the Violette & Samuel Glasstone Research Fellowships in Science, and NSERC (S.A.L.R.) for generous financial support, as well as the EPSRC UK Mass Spectrometry Facility at Swansea University for mass spectra.

■ REFERENCES

- (1) (a) Liu, Z.; Tian, C.; Yu, J.; Li, Y.; Jiang, W.; Mao, C. *J. Am. Chem. Soc.* **2015**, *137*, 1730. (b) Day, A. I.; Blanch, R. J.; Arnold, A. P.; Lorenzo, S.; Lewis, G. R.; Dance, I. *Angew. Chem., Int. Ed.* **2002**, *41*, 275. (c) Sun, B.; Wang, M.; Lou, Z.; Huang, M.; Xu, C.; Li, X.; Chen, L.-J.; Yu, Y.; Davis, G. L.; Xu, B.; Yang, H.-B.; Li, X. *J. Am. Chem. Soc.* **2015**, *137*, 1556. (d) Iwanaga, T.; Nakamoto, R.; Yasutake, M.; Takemura, H.; Sako, K.; Shimmyozu, T. *Angew. Chem., Int. Ed.* **2006**, *45*, 3643. (e) Danjo, H.; Hashimoto, Y.; Kidena, Y.; Nogamine, A.; Katagiri, K.; Kawahata, M.; Miyazawa, T.; Yamaguchi, K. *Org. Lett.* **2015**, *17*, 2154. (f) Kawase, T.; Tanaka, K.; Shiono, N.; Seirai, Y.; Oda, M. *Angew. Chem., Int. Ed.* **2004**, *43*, 1722. (g) Dalgarno, S. J.; Atwood, J. L.; Raston, C. L. *Chem. Commun.* **2006**, 4567.
- (2) (a) Chichak, K. S.; Cantrill, S. J.; Pease, A. R.; Chiu, S.-H.; Cave, G. W. V.; Atwood, J. L.; Stoddart, J. F. *Science* **2004**, *304*, 1308. (b) Loren, J. C.; Yoshizawa, M.; Haldimann, R. F.; Linden, A.; Siegel, J. S. *Angew. Chem., Int. Ed.* **2003**, *42*, 5702. (c) Forgan, R. S.; Wang, C.; Friedman, D. C.; Spruell, J. M.; Stern, C. L.; Sarjeant, A. A.; Cao, D.; Stoddart, J. F. *Chem. - Eur. J.* **2012**, *18*, 202.
- (3) Hervieu, M.; Mellène, B.; Retoux, R.; Boudin, S.; Raveau, B. *Nat. Mater.* **2004**, *3*, 269.
- (4) Lu, X.; Li, X.; Guo, K.; Wang, J.; Huang, M.; Wang, J.-L.; Xie, T.-Z.; Moorefield, C. N.; Cheng, S. Z. D.; Wesdemiotis, C.; Newkome, G. R. *Chem. - Eur. J.* **2014**, *20*, 13094.
- (5) (a) Ueno, H.; Nishihara, T.; Segawa, Y.; Itami, K. *Angew. Chem., Int. Ed.* **2015**, *54*, 3707. (b) Iwamoto, T.; Slanina, Z.; Mizorogi, N.; Guo, J.; Akasaka, T.; Nagase, S.; Takaya, H.; Yasuda, N.; Kato, T.; Yamago, S. *Chem. - Eur. J.* **2014**, *20*, 14403.
- (6) (a) O'Sullivan, M. C.; Sprafke, J. K.; Kondratuk, D. V.; Rinfray, C.; Claridge, T. D. W.; Saywell, A.; Blunt, M. O.; O'Shea, J. N.; Beton, P. H.; Malfois, M.; Anderson, H. L. *Nature* **2011**, *469*, 72. (b) Sprafke, J. K.; Kondratuk, D. V.; Wykes, M.; Thompson, A. L.; Hoffmann, M.; Drevinskas, R.; Chen, W. H.; Yong, C. K.; Karnbratt, J.; Bullock, J. E.; Malfois, M.; Wasielewski, M. R.; Albinsson, B.; Herz, L. M.; Zigmantas, D.; Beljonne, D.; Anderson, H. L. *J. Am. Chem. Soc.* **2011**, *133*, 17262. (c) Kondratuk, D. V.; Perdigo, L. A.; Esmail, A. M. S.; O'Shea, J. N.; Beton, P. H.; Anderson, H. L. *Nat. Chem.* **2015**, *7*, 317.
- (7) Jiang, H.-W.; Tanaka, T.; Mori, H.; Park, K. H.; Kim, D.; Osuka, A. *J. Am. Chem. Soc.* **2015**, *137*, 2219.
- (8) (a) Nakamura, Y.; Aratani, N.; Osuka, A. *Chem. Soc. Rev.* **2007**, *36*, 831. (b) Yang, J.; Yoon, M.-C.; Yoo, H.; Kim, P.; Kim, D. *Chem. Soc. Rev.* **2012**, *41*, 4808.
- (9) (a) Parkinson, P.; Knappke, C. E. I.; Kamonsutthipajit, N.; Sirithip, K.; Matichak, J. D.; Anderson, H. L.; Herz, L. M. *J. Am. Chem. Soc.* **2014**, *136*, 8217. (b) Yong, C.-K.; Parkinson, P.; Kondratuk, D. V.; Chen, W.-H.; Stannard, A.; Summerfield, A.; Sprafke, J. K.; O'Sullivan, M. C.; Beton, P. H.; Anderson, H. L.; Herz, L. M. *Chem. Sci.* **2015**, *6*, 181. (c) Parkinson, P.; Kondratuk, D. V.; Menelaou, C.; Gong, J. Q.; Anderson, H. L.; Herz, L. M. *J. Phys. Chem. Lett.* **2014**, *5*, 4356.
- (10) (a) Kuramochi, Y.; Sandanayaka, A. S. D.; Satake, A.; Araki, Y.; Ogawa, K.; Ito, O.; Kobuke, Y. *Chem.-Eur. J.* **2009**, *15*, 2317. (b) Satake, A.; Azuma, S.; Kuramochi, Y.; Hirota, S.; Kobuke, Y. *Chem.-Eur. J.* **2011**, *17*, 855.
- (11) Cogdell, R. J.; Gall, A.; Köhler, J. Q. *Rev. Biophys.* **2006**, *39*, 227.
- (12) (a) Durot, S.; Taesch, J.; Heitz, V. *Chem. Rev.* **2014**, *114*, 8542. (b) Beletskaya, I.; Tyurin, V. S.; Tsivadze, A. Y.; Guillard, R.; Stern, C. *Chem. Rev.* **2009**, *109*, 1659.
- (13) (a) Kumar, P. P.; Maiya, B. G. *New J. Chem.* **2003**, *27*, 619. (b) Davidson, G. J. E.; Tong, L. H.; Raithby, P. R.; Sanders, J. K. M. *Chem. Commun.* **2006**, *29*, 3087. (c) Davidson, G. J. E.; Lane, L. A.; Raithby, P. R.; Warren, J. E.; Robinson, C. V.; Sanders, J. K. M. *Inorg. Chem.* **2008**, *47*, 8721.
- (14) (a) Cohen, Y.; Avram, L.; Frish, L. *Angew. Chem., Int. Ed.* **2005**, *44*, 520. (b) Avram, L.; Cohen, Y. *Chem. Soc. Rev.* **2015**, *44*, 586.
- (15) Hogben, H. J.; Sprafke, J. K.; Hoffmann, M.; Pawlicki, M.; Anderson, H. L. *J. Am. Chem. Soc.* **2011**, *133*, 20962.
- (16) Hunter, C. A.; Anderson, H. L. *Angew. Chem., Int. Ed.* **2009**, *48*, 7488.
- (17) Kondratuk, D. V.; Perdigo, L. M. A.; O'Sullivan, M. C.; Svatek, S.; Smith, G.; O'Shea, J. N.; Beton, P. H.; Anderson, H. L. *Angew. Chem., Int. Ed.* **2012**, *51*, 6696.
- (18) Sprafke, J. K.; Odell, B.; Claridge, T. D. W.; Anderson, H. L. *Angew. Chem., Int. Ed.* **2011**, *50*, 5572.
- (19) (a) Anderson, S.; Anderson, H. L.; Sanders, J. K. M. *Acc. Chem. Res.* **1993**, *26*, 469. (b) Zhu, B.; Chen, H.; Lin, W.; Ye, Y.; Wu, J.; Li, S. *J. Am. Chem. Soc.* **2014**, *136*, 15126. (c) Hoffmann, M.; Wilson, C. J.; Odell, B.; Anderson, H. L. *Angew. Chem., Int. Ed.* **2007**, *46*, 3122. (d) Liu, P.; Neuhaus, P.; Kondratuk, D. V.; Balaban, T. S.; Anderson, H. L. *Angew. Chem., Int. Ed.* **2014**, *53*, 7770. (e) Liu, S.; Kondratuk, D. V.; Rousseaux, S. A. L.; Gil-Ramírez, G.; O'Sullivan, M. C.; Cremers, J.; Claridge, T. D. W.; Anderson, H. L. *Angew. Chem., Int. Ed.* **2015**, *54*, 5355.
- (20) (a) Mayor, M.; Didschies, C. *Angew. Chem., Int. Ed.* **2003**, *42*, 3176. (b) May, R.; Jester, S.-S.; Höger, S. *J. Am. Chem. Soc.* **2014**, *136*, 16732. (c) Sun, Q.-F.; Iwasa, J.; Ogawa, D.; Ishido, Y.; Sato, S.; Ozeki, T.; Sei, Y.; Yamaguchi, K.; Fujita, M. *Science* **2010**, *328*, 1144.